

ORIGINAL PAPER

Hong Shen · James E. Mark · Carl J. Seliskar
Harry B. Mark, Jr. · William R. Heineman

Blocking behavior of self-assembled monolayers on gold electrodes

Received: 16 January 1997 / Accepted: 4 March 1997

Abstract Self-assembled monolayers (SAMs) with metal electrodes, especially thiols on gold, are the subject of this investigation because of the unique properties of SAM-modified surfaces. Normal alkanethiols are used to modify the surface of a conventional gold electrode to block certain ions such as Pb(II) and Cu(II) from the surface of the electrode. Normal alkanethiols are also used to study the SAM-gold interfacial adsorption-desorption behavior of the self-assembled monolayer. The effects of varying chain length of SAMs, varying concentration of the alkanethiol solutions, immersion time of the pure gold electrode in the SAM solution, and the stability of a SAM-modified gold electrode in fresh chloroform are investigated using the oxidation-reduction peaks of gold. Conditions that optimize the surface coverage and the uniformity of the SAMs have been determined. Normal alkanethiols proved to be a good insulator on the electrode surface.

Key words Self-assembled monolayers · Thiols · Gold · Electrode · Adsorption

Introduction

There is considerable interest in the synthesis and properties of well-organized mono- and multilayer molecular thin films. These films are usually formed by the Langmuir-Blodgett (LB) method of thin film transfer from solvent to substrate [1, 2], by “self-assembly” chemisorption, and by vapor deposition (see [3] and references therein). Self-assembly chemisorption is a process by which an oriented monolayer film forms on a surface by the spontaneous adsorption of molecules from solution. It is the most promising strategy for

constructing stable, well-defined monolayers on electrode surfaces. Molecules that adsorb strongly to a surface and have shapes that pack well in two dimensions are used to form SAMs. Chemical systems that exhibit self-assembly include thiols, disulfides, and sulfides on gold [4–40], silanes on silicon dioxides [41–49], fatty acids on metal oxide surfaces [50, 51], phosphonates on phosphonate surfaces [52], and isocyanides on platinum [53]. Of all the types of self-assembled monolayers that have been studied [52], two systems have shown the greatest promise for providing an organic surface with a uniform chemical structure: adsorption of organosulfur compounds on noble metals such as gold [12, 31, 39, 54] and silver and reaction of alkyltrichlorosilanes with silicon or glass [41–47]. Exposure of a gold surface to a dilute (1.0 mM) solution of an *n*-alkanethiol results in a chemisorbed monolayer that is densely packed in two dimensions and excludes ions and water from the underlying gold [12, 17, 18]. The thermodynamically favorable formation of the gold-thiolate bond makes the gold-thiol system ideal for monolayer self-assembly schemes, and the stability of that bond over a wide range of applied potential makes such a system suitable for electrochemical studies. Self-assembly chemistry offers advantages over other approaches to electrode surface modification such as polymer films, which are usually much thicker and have considerable tertiary structure, and transferred LB films, which often contain many defects and can be intrinsically unstable.

SAMs are versatile model systems for studying interfacial electron transfer, biological interactions, molecular recognition, double-layer structure, adhesion, and other interfacial phenomena [55–58]. SAMs can produce a variety of structures with different types of surface functional groups and with varied topography [59]. Such structural flexibility suggests many future applications.

The SAMs can be divided into those that adhere to the substrate primarily via chemical reaction (chemisorption) and those that adhere primarily via long range forces

Hong Shen · James E. Mark · Carl J. Seliskar
Harry B. Mark, Jr. · William R. Heineman (✉)
Department of Chemistry, University of Cincinnati,
P.O. Box 210172, Cincinnati, OH 45221-0172, USA

(physisorption). The latter always involve crosslinked molecules for film stability and are exemplified by alkylsiloxanes [60]. The chemisorbed SAMs can be divided further into those that form superlattices of the substrate structure, exemplified by alkanethiols on Au [58] and those that do not. The latter in turn can be divided into cases with covalent and ionic type bonding [50, 51].

The majority of cases studied has involved assembly of normal alkyl chain-based molecules. The primary reason for this is the ease with which alkyl chains self-organize, as is widely manifested in biological structures involving lipid molecules. Further, these types of molecules are generally surfactants and, as such, the SAM structures are closely related to the traditional LB structures that have been studied for many years.

Our goal in this paper is to study the adsorption behavior of normal alkanethiols on gold electrodes in order to optimize the coverage and organization of the monolayer. One hypothesis is supported by the results herein: SAM monolayers formed from alkanethiols are remarkably stable as electrode coatings. The known affinity of sulfur for gold [61] accounts for the increased stability. Furthermore, the alkanethiols form monolayers that are so compact that electrochemical processes, such as gold oxidation, are strongly suppressed. In such circumstances it becomes possible to investigate electron transfer by tunneling across the monolayer.

Experimental

Reagents

Normal alkanethiols and *tris*-(2,2'-bipyridyl)-ruthenium(II) chloride hexahydrate were purchased from Aldrich Chemicals (Milwaukee, Wis.). Concentrated sulfuric acid, chloroform, lead nitrate, copper nitrate and ascorbic acid were purchased from Fisher Scientific (Fair Lawn, N.J.). All reagents were analytical grade. Gold disk electrodes (surface area $A = 2.01 \text{ mm}^2$) were obtained from Bioanalytical Systems (West Lafayette, Ind.) and Fibremet polishing disks (Buehler, Lake Bluff, Ill.) were used to polish the electrode surface. Water was purified with a Barnstead Nano-pure water system.

Apparatus

Cyclic voltammetry (CV) and linear sweep stripping voltammetry experiments were conducted with a BAS-100B/W system. The electrochemical cell consisted of a BAS Ag/AgCl, 3 M NaCl reference electrode, a platinum auxiliary electrode and a bare or SAM-modified gold working electrode.

SAM solution preparation

All SAM solutions were prepared by dissolving the thiol in pure chloroform at room temperature.

Electrode preparation

The gold electrodes were first polished on a 3- μm silicon carbide disk followed by a 0.3- μm aluminum oxide disk, followed by

dipping into Piranha solution (1:3 H_2O_2 : H_2SO_4 , which reacts with organic compounds violently and should be used with extreme care) for 30 s to remove organic compounds that might have adsorbed on the gold electrode surface. The gold electrodes were rinsed with organic-free water and dried under N_2 in a glove box. The gold electrodes were cycled in 0.5 M H_2SO_4 aqueous solution from -200 mV to 1400 mV vs Ag/AgCl until a stable voltammogram was obtained. Following the cycling, the gold electrodes were rinsed with organic-free water and dried under N_2 again before the self-assembling process.

Electrode modification

The gold electrodes were immersed in 50 mM SAM chloroform solution for 30 min to form a monolayer on the surface and then rinsed with fresh chloroform to remove any thiol residues on the surface. All the modifications were done at room temperature.

Electrode evaluation

CV was performed from 1400 mV to 200 mV vs Ag/AgCl using the SAM-modified electrodes in supporting electrolyte solution, which was 0.5 M H_2SO_4 , to investigate the degree of coverage of the gold surface by the monolayer. All experiments were performed under ambient conditions. Solutions were purged with argon before measurements and blanketed with argon during measurements. The peak current, i_p , was measured as the distance along a vertical line from the peak to intersection with a baseline that was drawn to intersect tangentially with the voltammogram on either side of the wave.

Results

Figure 1 shows the suppression of gold reduction/oxidation by a SAM in 0.5 M H_2SO_4 . Curve A is a CV for bare gold electrode reduction/oxidation. A broad oxidation wave between $+1100 \text{ mV}$ and $+1400 \text{ mV}$ vs Ag/AgCl represents the formation of gold oxide on the electrode surface. When the potential scan is reversed there is a sharp cathodic peak in the range of $+1000 \text{ mV}$ to $+800 \text{ mV}$ vs Ag/AgCl representing the

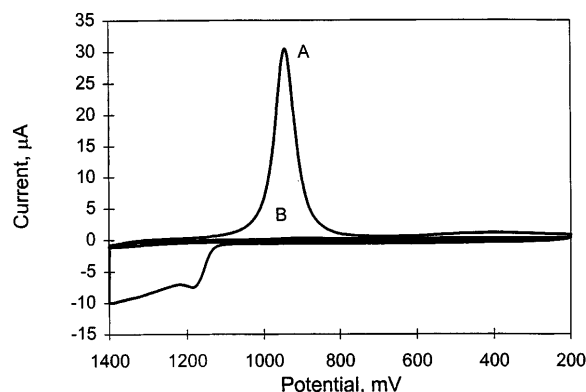


Fig. 1 Cyclic voltammograms of gold electrode (A) bare and (B) modified with 1-dodecanethiol in 0.5 M H_2SO_4 . SAM formed in 0.05 M thiol chloroform solution, 30-min immersion. CV scan from 1400 mV to 200 mV vs Ag/AgCl, 100 mV/s

reduction of gold oxide on the electrode surface. The peak current for the gold oxide reduction is $+29.2 \mu\text{A}$. When the same gold electrode was modified by 1-dodecanethiol, both of the gold oxide peaks are significantly depressed, as seen in curve B in Fig. 1. The reduction peak current was calculated as $+0.179 \mu\text{A}$. The SAM modification on the surface of the gold electrode suppressed the gold oxide reduction peak by two orders of magnitude with respect to that of the bare gold electrode in the same supporting electrolyte solution. The voltammogram stays the same during repeated scans. The optimization of the SAM system for suppression in terms of the thiol chain length, thiol solution concentration and immersion time of gold electrode in the thiol solution for maximum inhibition of gold oxide formation and for maximum stability of the monolayer in various solvent systems is discussed below. The normal alkanethiol can also be used as an insulating material to block certain electrochemical reactions in addition to the gold oxide formation discussed above.

SAM chain length

Figure 2 shows the effect of optimizing the surface coverage of the gold electrode modified with six different normal alkanethiols, $\text{HS}(\text{CH}_2)_n\text{CH}_3$ ($n = 4, 6, 8, 11, 15, 17$). The gold oxide reduction peak area is plotted versus the total number of carbon atoms (representing the chain length) in the alkanethiol. The degree of surface coverage can be determined through the decrease in the area associated with the reduction of gold oxide on the electrode surface [18, 22]. We use the term surface coverage to mean physical covering of the electrode surface by alkanethiol chains rather than a "concentration" of the alkanethiol on the surface. It can be seen that the surface coverage, i.e., the peak area,

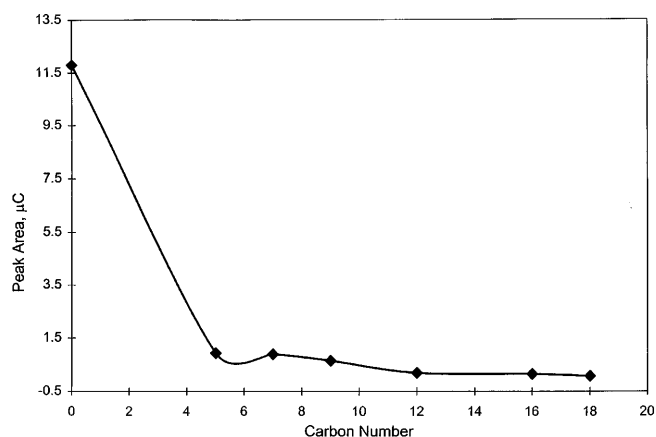


Fig. 2 Effect of chain length of *n*-alkanethiols on gold oxide reduction peak in 0.5 M H_2SO_4 . *N*-alkanethiol $\text{HS}(\text{CH}_2)_n\text{CH}_3$ ($n = 4, 6, 8, 11, 15, 17$), 0.05 M in chloroform, 30-min immersion. CV from $+1400 \text{ mV}$ to 200 mV vs Ag/AgCl , scan rate 100 mV/s

is inversely proportional to the length of the thiol. Thus, the surface coverage increases as the thiol chain length increases. The peak area decreases from $11.7 \mu\text{C}$ for the bare gold electrode (0 carbons) to $0.929 \mu\text{C}$ for gold electrodes modified with 1-pentanethiol (5 carbons) and to $0.0728 \mu\text{C}$ for gold electrodes modified with octadecyl mercaptan (18 carbons). This represents surface coverage increases from 0.00 to 92% and 99%, respectively. The peak area essentially levels off when the carbon number reaches 12. Under the conditions in Fig. 2, the short chain thiols do not form well-defined monolayers. Also they are not sufficiently hydrophobic to block the interaction between the gold surface and the solvent-supporting electrolyte. On the other hand, 1-dodecanethiol and those thiols that have longer hydrophobic chains can be used as insulating materials to virtually block off such a surface electrochemical process. This behavior agrees with that reported for C_3 , C_6 , and C_{11} [62], and C_{12} – C_{18} alkanethiols [18].

Thus, longer alkyl groups have stronger hydrophobic interactions resulting in electrode surfaces that are more highly organized. That is, longer thiols form better organized self-assembled monolayers which are defect-free and are better at blocking the access of solvent-supporting electrolyte to the electrode surface. However, there are usually some defects that can be considered pinholes in the monolayer. The existence and determination of such pinholes have been demonstrated electrochemically [12].

SAM solution concentration

Figure 3 shows the effect of thiol solution concentration on gold electrode surface coverage. The concentration of 1-dodecanethiol was varied from 10 mM to 100 mM in chloroform where all other parameters remained the

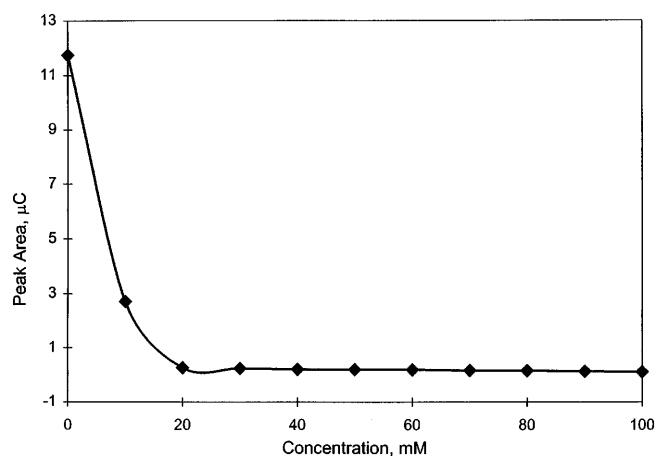


Fig. 3 Effect of concentration of *n*-alkanethiol on gold oxide reduction peak in 0.5 M H_2SO_4 . 1-dodecanethiol $\text{HS}(\text{CH}_2)_{11}\text{CH}_3$, from 0.05 M to 0.1 M in chloroform, 30-min immersion. CV from $+1400 \text{ mV}$ to 200 mV vs Ag/AgCl , scan rate 100 mV/s

same. It can be seen in Fig. 3 that as the thiol concentration increases the gold oxide reduction peak area decreases from 11.7 μC for bare gold electrode (0 mM) to 2.71 μC for 10 mM and to 0.0965 μC for a 100 mM thiol/chloroform solution. The surface coverage increases, from 0.00 to 77% and 99%, respectively. The peak area levels off at about 20 mM.

Immersion time

Figure 4 shows the effect of immersion time of the gold electrode in a 1-dodecanethiol solution. The immersion time was varied from 5 min to 60 min, and all other parameters remained the same. The gold oxide reduction peak area in Fig. 4 decreases, from 11.7 μC for bare gold electrode (0 min) to 0.496 μC for 5 min immersion and to 0.0876 μC for 60 min immersion of the gold electrode in the thiol chloroform solution. The surface coverage increases from 0.00 to 96% and 99%, respectively. The peak area levels off after 30 min of immersion. Increasing the immersion time beyond 30 min probably allows further ordering of the monolayer, even though it cannot be observed experimentally.

Stability of SAM in pure solvents

Figure 5 shows the effect that immersion of a 1-dodecanethiol-modified gold electrode in 25 ml of pure chloroform has on the gold oxide reduction peak. The immersion time was varied from 5 min to 60 min. The surface coverage decreases from 98% to about 80% after about 30 min, after which it remains constant. During the initial 30 min the thiol molecules on the electrode surface change their conformation to allow more exposure of substrate gold.

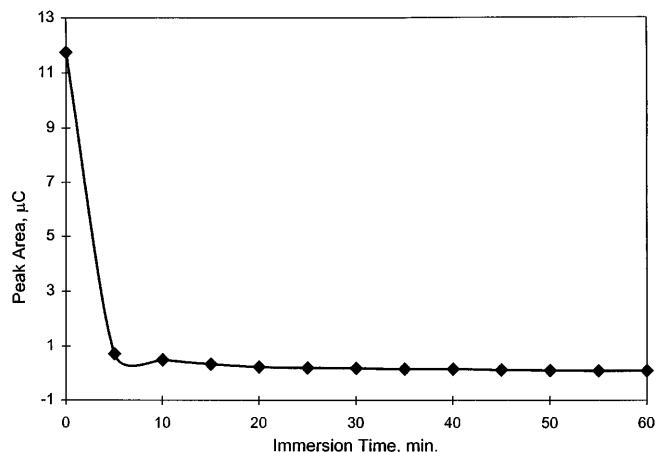


Fig. 4 Effect of immersion time of gold electrode in 1-dodecanethiol solution on gold oxide reduction peak in 0.5 M H_2SO_4 . 1-dodecanethiol $\text{HS}(\text{CH}_2)_{11}\text{CH}_3$, 0.05 M chloroform, immersion time from 5 min to 60 min. CV from +1400 mV to 200 mV vs Ag/AgCl, scan rate 100 mV/s

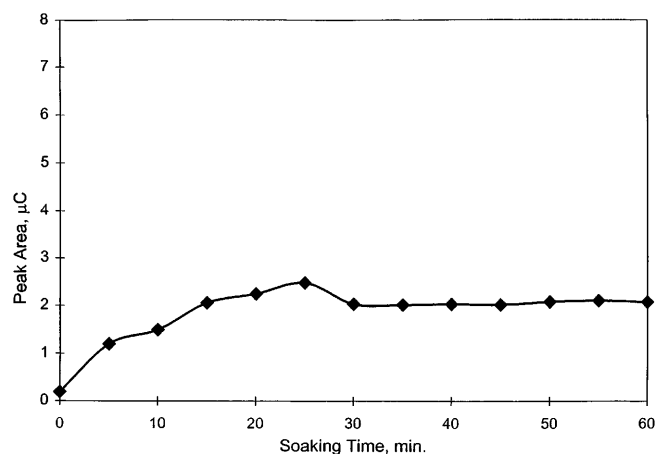


Fig. 5 Stability of 1-dodecanethiol self-assembled on gold electrode in fresh chloroform. 1-dodecanethiol $\text{HS}(\text{CH}_2)_{11}\text{CH}_3$, 0.05 M in chloroform, 30-min immersion. CVs were taken at 5-min intervals after immersion of the modified gold electrode in fresh chloroform, from +1400 mV to 200 mV vs Ag/AgCl, scan rate 100 mV/s

The same electrode can be dried and stored under room conditions for days and reused. After the monolayer equilibrates with solution, it is very stable. However, strong oxidants, such as NaClO , can remove the monolayer from the electrode surface by breaking the sulfur-gold bond and oxidizing the sulfur atoms.

The optimized self-assembly conditions are found to be 12-carbon chain length (1-dodecanethiol), 50 mM thiol concentration in chloroform and 30 min immersion of the electrode in the thiol chloroform solution. These conditions were used for the following studies.

N-alkanethiols blocking ascorbic acid

Figure 6 shows voltammograms of a gold electrode with and without SAM modification in 5 mM ascorbic acid, 0.5 M NaCl solution, at pH 7.0. At pH 7.0,

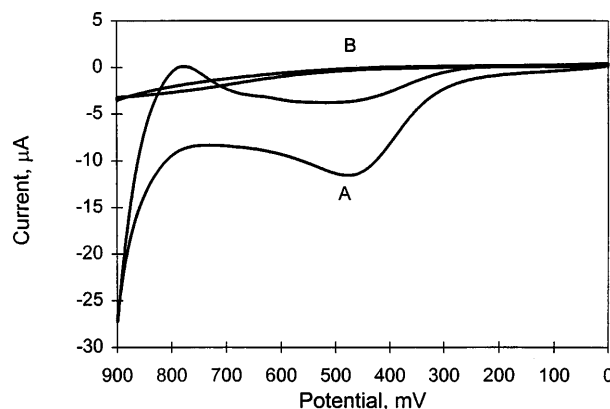


Fig. 6 Cyclic voltammograms of gold electrode (A) without and (B) with SAM modification in 5 mM ascorbic acid, 0.5 M NaCl solution at pH 7.0. SAM: hexadecyl mercaptan $\text{HS}(\text{CH}_2)_{15}\text{CH}_3$, 0.05 M in chloroform, 30-min immersion. CV from +900 mV to 0 mV vs Ag/AgCl, scan rate 100 mV/s

ascorbic acid is deprotonated to its ionized form, the ascorbate anion. The voltammogram at a bare gold electrode (curve A) shows the typical broad peak at about +450 mV for the oxidation of ascorbate. The voltammogram at a gold electrode modified with 1-dodecanethiol (curve B) shows the oxidation of ascorbate to be blocked by the self-assembled monolayer. The hydrophobicity of the 1-dodecanethiol self-assembled on the electrode surface prevents the ascorbate from diffusing through the monolayer and being oxidized at the surface of the electrode. Similar results were reported for a gold electrode modified with $\text{HS}(\text{CH}_2)_{10}\text{COOH}$ [62].

N-alkanethiols blocking $\text{Ru}(\text{bipy})_3^{2+}$

Figure 7 shows voltammograms of a gold electrode with and without SAM modification in 2.8×10^{-3} M $\text{Ru}(\text{bipy})_3^{2+}$, 0.1 M KCl solution. A well-defined CV, with a cathodic peak at +1040 mV and an anodic peak at +1100 mV, is obtained at the bare gold electrode (curve A), whereas both peaks disappeared when the electrode was modified by the self-assembled monolayer of 1-dodecanethiol (curve B). The charged $\text{Ru}(\text{bipy})_3^{2+}$ compound is blocked by the monolayer. Even though the compound is somewhat hydrophobic because of the aromatic ligands surrounding the ruthenium, it is difficult to transport this large dication to the electrode surface, which is well protected by the 1-dodecanethiol monolayer.

N-alkanethiols blocking Pb^{2+} and Cu^{2+}

Figure 8 shows the voltammograms of a gold electrode with and without SAM modification in 1 mM Pb^{2+} , 0.5 M KNO_3 solution at pH 3. The voltammogram at a bare gold electrode shows two anodic stripping peaks of

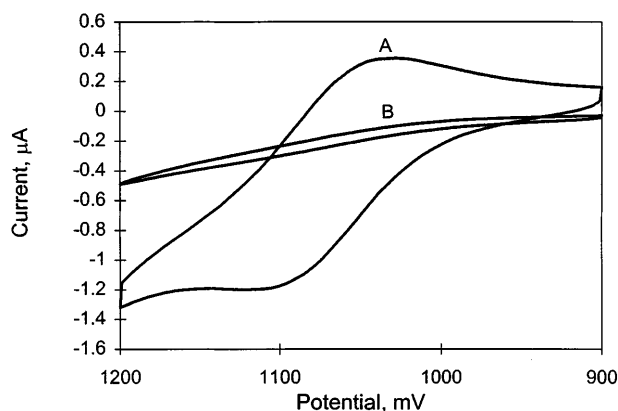


Fig. 7 Cyclic voltammograms of gold electrode (A) without and (B) with SAM modification in $2.8 \text{ mM } \text{Ru}(\text{bipy})_3^{2+}$, 0.1 M KCl solution at pH 7.0. SAM: 1-dodecanethiol $\text{HS}(\text{CH}_2)_{11}\text{CH}_3$, 0.05 M in chloroform, 30-min immersion. CV from +1200 mV to +900 mV vs Ag/AgCl, scan rate 100 mV/s

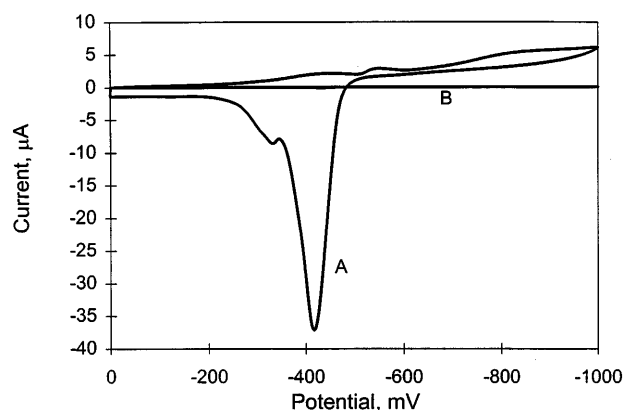


Fig. 8 Cyclic voltammograms of gold electrode (A) without and (B) with SAM modification in 1 mM $\text{Pb}(\text{NO}_3)_2$, 0.5 M KNO_3 solution at pH 3.0. SAM: hexadecyl mercaptan $\text{HS}(\text{CH}_2)_{15}\text{CH}_3$, 0.05 M in chloroform, 30-min immersion. CV from 0 mV to -1000 mV vs Ag/AgCl, scan rate 100 mV/s

Pb^0 from the electrode surface (curve A). The smaller peak at about -340 mV is the stripping of the first monolayer of lead on the gold electrode surface. (Underpotential deposition (UPD) effects [63] are common in stripping analysis at solid electrodes [64].) When the gold electrode was modified with hexadecyl mercaptan, the reduction of Pb^{2+} was blocked by the neutral, hydrophobic organic monolayer on the surface of the electrode (curve B).

The same phenomenon can also be found in Fig. 9, which shows the voltammograms of a gold electrode with and without SAM modification in 1 mM Cu^{2+} , 0.5 M KNO_3 solution at pH 3. Again, curve A in Fig. 9 is the voltammogram at a bare gold electrode. The cathodic peak at -300 mV is the reduction peak of Cu^{2+} to Cu^0 , and the sharp anodic peak at +100 mV is the stripping peak of the elemental Cu from the surface of electrode. The UPD effects are also evident in this voltammogram where a second Cu stripping peak is

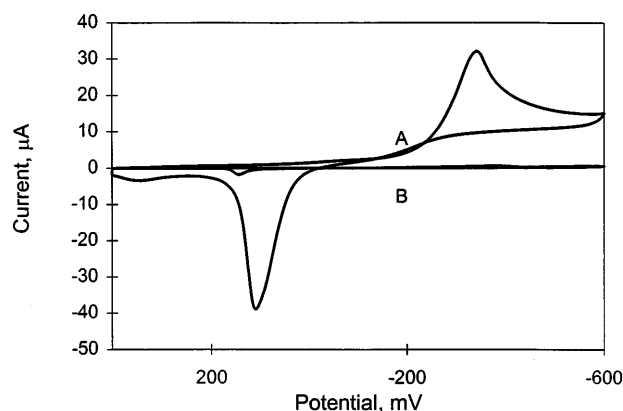


Fig. 9 Cyclic voltammograms of gold electrode (A) without and (B) with SAM modification in 1 mM $\text{Cu}(\text{NO}_3)_2$, 0.5 M KNO_3 solution at pH 3.0. SAM: hexadecyl mercaptan $\text{HS}(\text{CH}_2)_{15}\text{CH}_3$, 0.05 M in chloroform, 30-min immersion. CV from +400 mV to -600 mV vs Ag/AgCl, scan rate 100 mV/s

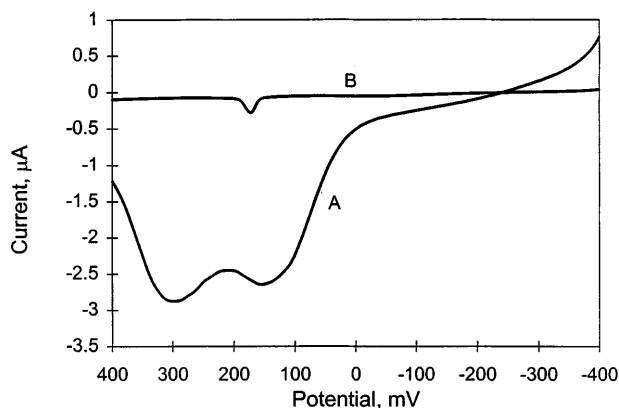


Fig. 10 Linear scan stripping voltammograms of gold electrode (A) without and (B) with SAM modification in $1 \mu\text{M}$ $\text{Cu}(\text{NO}_3)_2$, 0.5 M KNO_3 solution at pH 3.0. SAM: hexadecyl mercaptan $\text{HS}(\text{CH}_2)_{15}\text{CH}_3$, 0.05 M in chloroform, 30-min immersion. Deposition potential -400 mV , deposition time 250 s , scan from -400 mV to $+400 \text{ mV}$ vs Ag/AgCl , scan rate 100 mV/s

observed at $+350 \text{ mV}$. When the electrode was modified with hexadecyl mercaptan, the reduction of Cu^{2+} is almost totally blocked by the SAM monolayer. The small anodic peak at $+180 \text{ mV}$ in the voltammogram B represents the oxidation of some Cu^0 that has formed on the electrode surface. This is the result of defect pinhole sites in the monolayer allowing some Cu^{2+} ions to reach the gold electrode surface where it is reduced to form multilayer deposits.

Similarly, Fig. 10 shows stripping voltammograms of a gold electrode with and without SAM modification in $1 \mu\text{M}$ Cu^{2+} , 0.5 M KNO_3 at pH 3. The UPD effects are easily seen for this diluted Cu^{2+} solution in the voltammogram at a bare gold electrode (curve A). Instead of one sharp stripping peak of Cu, there are two overlapping peaks, one at $+310 \text{ mV}$ for the monolayer Cu stripping and one at $+160 \text{ mV}$ for the bulk Cu stripping. Curve B for a SAM-modified electrode shows a small Cu^0 stripping peak at potential $+170 \text{ mV}$ for bulk Cu stripping from deposits formed in pinholes. Again, with SAM modification by hexadecyl mercaptan, the reduction of Cu^{2+} at potentials more negative than -200 mV is greatly attenuated (curve B).

Conclusions

The surface coverage and uniformity of the SAM system of normal alkanethiol on gold electrodes have been optimized in terms of thiol chain length, thiol solution concentration, and immersion time of the gold electrode in the thiol solution. The gold oxide reduction peak was used to evaluate the SAM-gold system by using peak areas to quantify surface coverage and organization. The 12-carbon chain length, 50 mM concentration in chloroform, and 30 min immersion were found to be the optimum conditions to form a well-oriented

monolayer on the electrode surface. Once the thiol assembled on the electrode surface, it was quite stable over a long time and over a large range of applied potential. Normal alkanethiols form hydrophobic monolayers on the gold electrode surface which prevent charged ions from approaching the electrode surface for oxidation/reduction.

Acknowledgements The authors gratefully acknowledge support provided by the Department of Energy (Grant DE-FG07-96 ER62311).

References

- Robert G (ed) (1990) Langmuir-Blodgett films. Plenum, New York
- Ulman A (1991) Ultrathin organic films. Academic Press, San Diego
- Ulman A (1991) Adv Mater 3: 298
- Chidsey CED, Bertozzi CR, Putvinski TM, Muijsce AM (1990) J Am Chem Soc 112: 4301
- Creager SE, Rowe GK (1991) Anal Chim Acta 246: 233
- Chidsey CED (1991) Science 251: 919
- Collard DM, Fox MA (1991) Langmuir 7: 1192
- Buttry D (1990) Langmuir 6: 1319
- Creager SE, Collard DM, Fox MA (1990) Langmuir 6: 1617
- Soriaga MP, Bravo BJ, Michelhaugh SL (1988) J Electroanal Chem: Interfacial Electrochem 241: 199
- Obeng YS, Bard AJ (1991) Langmuir 7: 195
- Porter MD, Bright TB, Allara DL, Chidsey CED (1987) J Am Chem Soc 109: 3559
- Trevor DJ, Chidsey CED, Loiancono DN (1989) Phys Rev Lett 62 (8): 9295
- Wiechers J, Twomey T, Kolb DM (1988) J Electroanal Chem: Interfacial Electrochem 248: 451
- Chidsey CED, Loiancono DN (1990) Langmuir 6: 682
- Chidsey CED, Liu GY, Rowntree P, Scoles G (1989) J Chem Phys 91: 4421
- Chidsey CED, Liu GY, Scoles G, Wang J (1990) Langmuir 6: 1804
- Finklea HO, Avery S, Lynch M, Furttsch T (1987) Langmuir 3: 409
- Finklea HO, Snider DA, Fedyk J (1990) Langmuir 6: 371
- Sabatani E, Rubinstein I, Maoz R, Sagiv J (1987) J Electroanal Chem: Interfacial Electrochem 219: 365
- Sabatani E, Rubinstein I (1987) J Phys Chem 91: 6663
- Rubinstein I, Steinberg S, Tor Y, Shanzer A, Sagiv J (1988) Nature 332: 426
- Fabianowski W, Coyle LC, Weber BA, Granata RD, Castner DG, Sadownik A, Regen SL (1989) Langmuir 5: 35
- Bunding-Lee KA (1990) Langmuir 6: 709
- Barner BJ, Corn RM (1990) Langmuir 6: 1023
- Nuzzo RG, Fusco FA, Allara DL (1987) J Am Chem Soc 109: 2358
- Nozzo RG, Dubois LH, Allara DL (1990) J Am Chem Soc 112: 558
- Dubois LH, Zegarski BR, Nuzzo RG (1990) J Am Chem Soc 112: 570
- Dubois LH, Zegarski BR, Nuzzo RG (1987) Proc Natl Acad Sci USA 84: 4739
- Nuzzo RG, Zegarski BR, Dubois LH (1987) J Am Chem Soc 109: 733
- Bain CD, Troughton EB, Tao YT, Evall J, Whitesides GM, Nuzzo RG (1989) J Am Chem Soc 111: 321
- Whitesides GM, Laibinis PE (1990) Langmuir 6: 87
- Bain CD, Evall J, Whitesides GM (1989) J Am Chem Soc 111: 7155

34. Bain CD, Whitesides GM (1989) *J Am Chem Soc* 111: 7164
35. Bain CD, Whitesides GM (1989) *Angew Chem Intl Ed Engl* 28: 506
36. Bain CD, Biebuyck HA, Whitesides GM (1989) *Langmuir* 5: 723
37. Strong L, Whitesides GM (1988) *Langmuir* 4: 546
38. Bain CD, Whitesides GM (1988) *J Am Chem Soc* 110: 6560
39. Troughton EB, Bain CD, Whitesides GM, Nuzzo RG, Allara DL, Porter MD (1988) *Langmuir* 4: 365
40. Bain CD, Whitesides GM (1988) *Science* 24: 62
41. Sagiv J (1980) *J Am Chem Soc* 102: 92
42. Netzer L, Sagiv J (1983) *J Am Chem Soc* 105: 674
43. Maoz R, Sagiv J (1984) *J Colloid Interface Sci* 109: 465
44. Gun J, Iscovici R, Sagiv J (1984) *J Colloid Interface Sci.* 1984, 101, 201
45. Gun J, Sagiv JJ *Colloid Interface Sci* 112: 457
46. Maoz R, Sagiv J (1987) *Langmuir* 3: 1034
47. Maoz R, Sagiv J (1987) *Langmuir* 3: 1045
48. Tillman N, Ulman A, Penner PL (1989) *Langmuir* 5: 101
49. Tillman N, Ulman A, Schildkraut JS, Penner TL (1988) *J Am Chem Soc* 110: 6136
50. Allara DL, Nuzzo RG (1985) *Langmuir* 1: 45
51. Allara DL, Nuzzo RG (1985) *Langmuir* 1: 52
52. Lee H, Kepley LJ, Hong HG, Akhter S, Mallouk TE (1988) *J Phys Chem* 92: 2597
53. Hickman JJ, Zou C, Ofer D, Harvey PD, Wrighton MS, Labibinis PE, Bain CD, Whitesides GM (1989) *J Am Chem Soc* 111: 7271
54. Nuzzo RG, Allara DL (1983) *J Am Chem Soc* 105: 4481
55. Hussling L, Michel B, Ringsdorf H, Rohrer H (1992) *Angew Chem Intl Ed Engl* 30: 569
56. Bryant M, Crooks RM (1993) *Langmuir* 9: 385
57. Berndt P, Kurihara K, Kunitake T (1992) *Langmuir* 8: 2486
58. Dubois LH, Nuzzo RG (1992) *Annu Rev Phys Chem* 43: 437 and references therein
59. Allara DL (1995) *Biosensors & Bioelectronics* 10: 771
60. Parikh AN, Allara DL, Ben Azouz I, Rondelez F (1994) *J Phys Chem* 98: 7577
61. Chambers JQ (1978) In: Bard AJ (Ed) *Encyclopedia of electrochemistry of the elements*, Vol 12. Dekker, New York
62. Malem F, Mandler D (1993) *Anal Chem* 65: 37
63. Bard AJ, Faulkner LR (1980) *Electrochemical Methods: Fundamentals and Applications*. Wiley, New York
64. Perone SP (1963) *Anal Chem* 35: 2091